Available online at www.sciencedirect.com

ScienceDirect

Procedia Materials Science (2015) 000–000

Procedia Materials Science

www.elsevier.com/locate/procedia

International Congress of Science and Technology of Metallurgy and Materials, SAM – CONAMET 2014

Structural and magnetic changes induced by electron and ion irradiation on HOPG

Milagros Ávila[a], Lisandro Venosta[b], Noelia Bajales[b]* and Paula Bercoff[a,b]*

[a]*FaMAF – UNC, Av. Medina Allende s/n, Córdoba X5000HUA, Argentina*
[b]*IFEG – UNC - CONICET, Av. Medina Allende s/n, Córdoba X5000HUA, Argentina*

Abstract

In recent decades, many studies reported magnetism in carbon-based materials. This phenomenon was attributed to structural defects within the sample. Many authors showed an increase of magnetization in HOPG (Highly Oriented Pyrolytic Graphite) induced by proton bombardment, meanwhile the effect of electronic irradiation on the magnetic behavior has been unattended till now. The aim of this work is to contribute to the understanding of defect-induced effects on the structural and magnetic properties of graphite. For this purpose, we performed experiments of irradiation on HOPG with two different impinging projectiles –electrons and ions. The structural characterization of the bombarded samples was carried out by Raman spectroscopy. On both irradiated samples we identify the D band, associated to the disorder induced by bombardment, with significantly distinct contributions depending on the projectile type. In order to interpret Raman results, a theoretical model proposed by Ferrari et al. was used to classify the generated defects. The relationship between the induced damage and magnetization was evaluated by magnetic characterization measurements with a SQUID (Superconducting Quantum Interference Device). Our results suggest that electron bombardment produces a higher change in the magnetic order compared to the magnetization induced by ion bombardment.

Peer-review under responsibility of the Scientific Committee of SAM– CONAMET 2014.

Keywords: Graphite, Electron and ion irradiation, Structural defects, Ferromagnetism

* Corresponding author. Tel.: +54 -351- 433- 4051 ; fax: +54- 351- 433- 4051 .
E-mail address: bercoff@famaf.unc.edu.ar; bajalesluna@famaf.unc.edu.ar

Peer-review under responsibility of the Scientific Committee of SAM– CONAMET 2014.

1. Introduction

Hybridization of carbon atomic orbitals generates a unique condition for the construction of a wide variety of allotropic forms. For over 25 years, only two allotropes of carbon were recognized: diamond and graphite. This scene changed drastically with the discovery of fullerenes (O´brien et al., 1986), carbon nanotubes (Iijima, 1991) and graphene (Novoselov et al., 2004). These new nano-structures triggered a new interest in the study of physical and chemical properties of carbon-based materials, increasing the amount of researches focused on the study of the magnetic properties exhibited by carbonaceous systems.

Until the mid-twentieth century, carbon-based materials were considered as non-magnetic. Nevertheless, since the early 90s, different researchers reported small ferromagnetism signals in fullerenes molecules (Allemand et al.,1991) and in pyrolytic carbon (Mizogami et al.,1991). Thus, Kopelevich et al. (2000) studied the magnetic properties of graphitic materials and observed ferromagnetism in HOPG samples for a wide range of temperatures. Another work (Makarova et al., 2001) revealed strong magnetic signals in fullerenes molecules. These reports were convincing: ferromagnetism was observed in carbon-based materials. One of the first explanations was the influence of magnetic impurities on the observed induced magnetism (Talyzin et al., 2007). This controversy promoted meticulous studies with the goal of understanding the role of magnetic impurities in graphitic samples. Esquinazi et al. (2002) studied the correlation between magnetic parameters and iron concentration in different samples, and showed that this correlation does not exist within the experimental error.

In the last years, the scientific community has focused its interest on punctual defect-induced ferromagnetism. In fact, defects produce unpaired spins, prompting magnetic order. For example, it was observed that magnetization in HOPG (Xiaoxang et al., 2012) can be diminished by annealing. Given that heat in graphite reduces the presence of defects, this result suggests that ferromagnetism is related to the defects in the microscopic structure of HOPG. Furthermore, Esquinazi et al. (2003) corroborated that protonic bombardment in HOPG samples, within a certain range of energy, increments magnetization values.

Nowadays there are still many open questions about the effects of bombardment in graphite, and few researches concerning electronic irradiation. Krasheninnikov et al. (2010) studied how incident electrons interact with graphitic materials transferring energy via electron-electron and nucleus-electron dispersion. In the first case, it is necessary that the electron reaches 100 keV in order to remove a carbon atom of the structure, meanwhile electron-electron dispersion can generate damages due to local chemical reactions. Kotakoski et al. (2011) showed that electronic irradiation at 300 keV in bi-dimensional sheets of graphene produces expulsion and rotation in atom bonds and long irradiation with energy in the range of 80 – 100 keV produces the movement of vacancies and di-vacancies.

The aim of this work is to contribute to the understanding of the role of defects induced by electron and ion irradiation, comparing their effects on the structure and magnetism of HOPG.

Nomenclature

EPMA	Electron Probe Microanalysis
H	Magnetic field
Hc	Coercive field
HOPG	Highly Oriented Pyrolytic Graphite
I_D	Intensity of the D band in the Raman spectrum
I_G	Intensity of the G band in the Raman spectrum
M	Magnetization
M_S	Saturation magnetization
SE	Electron irradiated sample
SI	Ion irradiated sample
XRD	X ray diffraction

2. Materials and Methods

2.1. Sample preparation and experimental techniques

In its natural state, graphite is found as a disordered mineral. Pyrolysis is a common and effective technique to prepare highly oriented samples; HOPG is manufactured in this way. It is made up by a stacking pile of graphene sheets. This characteristic allows to practice exfoliation in order to obtain smooth and uniform surfaces. In this work, different samples of the same HOPG batch (ZYB quality) were used. Impurity levels reported by the manufacturer are less than 10 ppm. PIXE (Particle Induced X-Ray Emission) was performed in order to verify the absence of magnetic contaminants in the samples, using a Tandem NEC Pelletron 5SDH of 1.7 MeV, accurate in the ppm level. XRD was employed to corroborate the high orientation of the graphite crystals in the samples, using a Philips PW 3830 diffractometer. Raman spectroscopy monitored the disorder due the induced defects generated by irradiation. This is a well-known technique used to characterize the structure of graphitic materials (Pimenta et al., 2007) because of its high sensitivity on physical and chemical variations. In order to interpret the obtained Raman results, a theoretical model proposed by Ferrari et al. (2000) was used (see Section 2.2). Data acquisition was performed with a Horiba Jobin-Yvon LabRam HR Confocal using a λ=514 nm laser in the wavelength range 900-3500 cm^{-1}. For magnetic characterization of the samples, a Quantum Design SQUID (MPMS XL7) was used. The sensitivity of the equipment is in the order of 10^{-8} emu. Magnetic loops M(H) were obtained at 4K, with the magnetic field applied parallel to the main graphene layers axis.

Three samples were cut from one of the ZYB HOPG. By mechanical exfoliation, the surface became free of impurities, plane and uniform. “Pristine” HOPG is taken in the as-prepared state. Immediately after exfoliation, the second piece was introduced in the JEOL JXA 8230 Electron Probe Microprobe's vacuum chamber, and electron-beam irradiated. Irradiation was carried out at 25 keV, on a $5x10^4$ μm^2area, with a current of 0.5 μA, in a time interval of 8 hs. The electron irradiation dose was 1.73 $x10^{12}$ particles/μm^2. This sample was named SE. Once irradiated, EPMA was used to obtain the impurities concentration of the surface. The samples were kept inside the vacuum chamber until Raman spectroscopy was performed, and then stored under room conditions. In order to carry out a comparison analysis, a third piece was cut out from the HOPG batch and irradiated with a 3000 keV H^+ ion beam, of 2 mm diameter wide and a current of 7.7 nA. The total ion irradiation dose was 6 $x10^8$ particles/μm^2. This sample was named SI.

2.2. Theoretical model

The different types of graphitic materials can be classified according its structural order, from microcrystal to glassy carbon. The ratio sp^2/sp^3 of the amount of bonding types in the sample, sp^2 phase clustering, rings and chains and bonding disorder, are the factors governing the degree of graphitic ordering and the shape of the Raman spectrum. Ferrari and Robertson (2000) studied the relationship between the ratio of the D and G bands intensities and the G band position as a function of the structural order in a sample. They proposed a three-stage model which defines an amorphization path that goes from graphite to amorphous carbon, by studying the main effects on the evolution of the Raman spectra, described as follows:

Stage 1: From graphite to nanocrystalline graphite. The main structural change goes from a monocrystalline to a polycrystalline material with virtually no sp^3 sites. The D band appears and the ratio of intensities I_D/I_G increases. A second peak appears at 1620 cm^{-1} which merges with the G peak, resulting in a net increase of the later from 1581 to 1600 cm^{-1}.

Stage 2: From nanocrystalline graphite to amorphous carbon. Amorphous carbon arises with sp^2 bonding sites consisting of distorted sixfold rings (20% sp^3 at the most). The ratio I_D/I_G decreases with increasing amorphization. The G band becomes smooth and its position shifts from 1600 to 1510 cm^{-1}. No peaks are observed in the range 2400-3100 cm^{-1}.

Stage 3: From amorphous carbon to tetrahedral amorphous carbon. The sp^3 content rises from 20% to 85%, while the sp^2 sites change gradually from rings to chains. The ratio I_D/I_G is very low or zero. A shift of the G band position is observed from 1510 to 1570 cm^{-1}.

In order to interpret the results of the structural characterization, the model previously described was used to analyze the Raman spectra of the ion/electron irradiated HOPG samples.

3. Results and Discussion

The effects produced by electronic and ionic bombardment on the structure of HOPG were analyzed using Raman spectroscopy. The corresponding Raman spectra of both irradiated samples are compared in Figure 1, together with the Raman spectrum of pristine HOPG. All curves are normalized to I_G. The X-ray diffractogram (not shown) of HOPG before bombardment revealed high initial ordering in the samples. The planes (002), (004) and (006) were identified, with the expected intensities ratio for perpendicular irradiation.

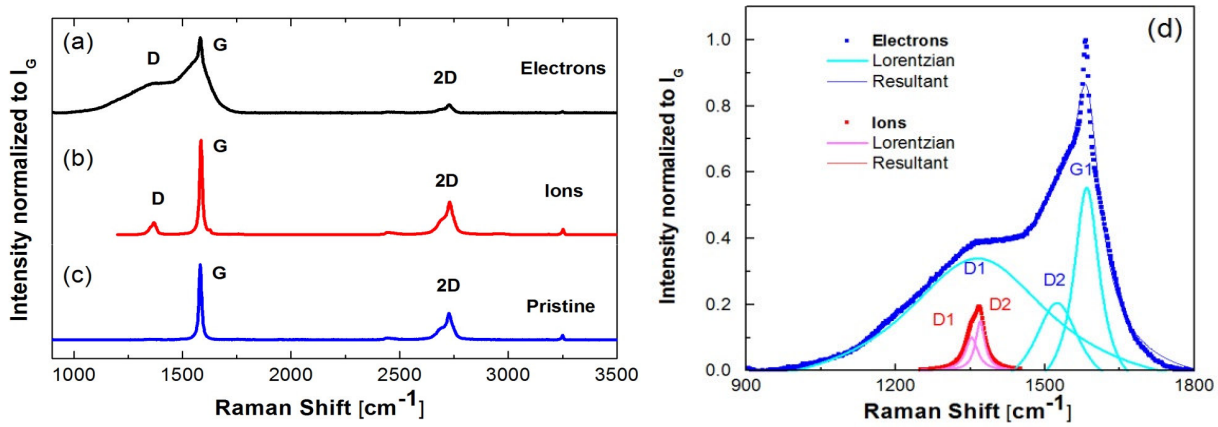

Figure1. Raman spectra of: (a) SE; (b) SI and (c) pristine HOPG. (d) D Band fitting of SE (blue online) and SI (red online).

Figure 1 (a-c) shows that G and 2D bands are present in all spectra, while the D band only appears in the irradiated samples. The shape of these bands depends on the impinging projectile. In fact, in the case of SI, the associated D peak is sharp and well separated from the adjacent G feature. In contrast, sample SE presents a wide D band, which is convoluted to the G band. It could be stated that irradiation with different particles yields defects on HOPG with well-differentiated characteristics. It is also observed that the 2D relative peak intensity for SE is weaker than that for SI. In order to compare quantitatively both irradiated samples spectra, the bands associated with disorder (D) were fitted by Lorentzian curves. The fitted peaks are shown in Figure 1(d) and the values obtained from the fits are listed in Table 1.

Table 1. Fitting parameters of the D band in SE and SI Raman spectra.

		D		G
		D1	D2	
Position (cm^{-1})	Ions (SI)	1350	1370	1583
	Electrons (SE)	1360	1525	1584
Intensity (*adimens.*)	Ions (SI)	0.10	0.15	1
	Electrons (SE)	0.34	0.20	0.55

In both irradiated samples, the D band is actually a doublet (D1 and D2), which is associated to the rupture of the space symmetry D^4_{6h} (D1) and to the disorder induced in boundaries (Compagnini et al., 1997).

Based on these results, the generated defects were classified according to the three-stage model described before. It is observed from the Raman spectra that I_D in SE is much larger than the corresponding for SI. This suggests that electron irradiation generates the kind of defects in HOPG which correspond to Stage 1. In this stage, the higher the intensity of the D peak, the lower the crystallinity of the graphite.

Regarding the stage corresponding to the defects in SI, a different approach can be made, following the work of Eckman et al. (2012). These authors were able to identify the type of defects generated in different HOPG samples by considering the I_D/I_G vs I_D'/I_G ratios. This ratio can take different values which can be related to the different kinds of defects that appear during Stage 1, when the concentration of defects remains low. They find that I_D/I_D'~13 is related to sp^3 sites in fluorinated graphene, I_D/I_D'~7 refers to vacancies in ion-bombarded graphene, and I_D/I_D'~3.5 to boundary-like defects in graphite.

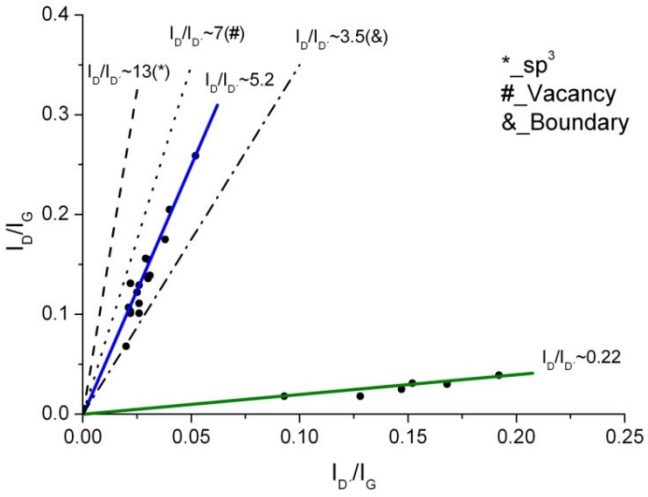

Figure 2: Linear dependence of I_D/I_D' in sample SI. The dots represent the measured values in this work, while the dashed an dotted lines are taken from reference (Eckmann et al., 2012).

The results of I_D/I_G as a function of I_D'/I_G for SI are shown as black dots in Figure 2, while the dashed, dotted and dash-dotted lines are the results from ref. (Eckmann et al., 2012). We find that the values of I_D/I_D' for SI group in two regions along two well-differenced lines, one with I_D/I_D'~5.2 and the other with I_D/I_D'~0.22. The first value is in between the reported values for vacancies and boundary defects and the second might be attributed to the bonds in graphite. Further experiments are necessary in order to completely understand this effect, but a link between the appearance of the doublet D1 and D2 and the two lines in I_D/I_G vs I_D'/I_G shouldn't be disregarded.

Figure 3(left) shows the ferromagnetic behavior of samples SI and SE at T=4K, after subtracting the strong diamagnetic contribution, typical of graphite. The loops are normalized to their respective saturation magnetization values Ms, for proper comparison. From the fitted ferromagnetic curves (not shown) the values obtained for the coercivities are 16 mT (SI), 43 mT (SE) and 3 mT (pristine). A larger increase in coercivity is observed in the electron-irradiated sample SE when compared to the ion-irradiated one, which leads to inferring that the kind of defects produced with electron-bombardment are more prone to induce a ferromagnetic order than the defects produced by ions on HOPG. Figure 3 (right) shows PIXE spectra after irradiation, where only Al (250 ± 50) ppm is detected. Therefore, a possible ferromagnetic contribution due to impurities is discarded.

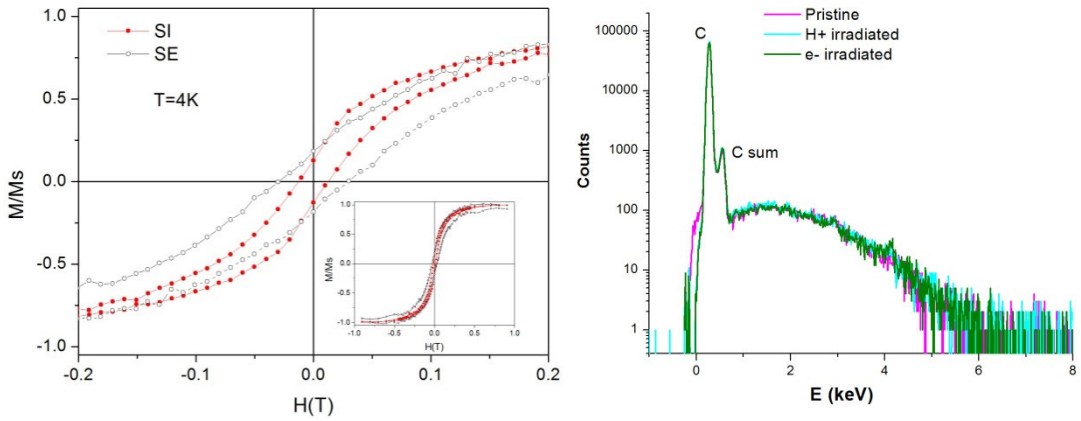

Figure 3: (Left) Hysteresis loop for: (a) SE (electrons); (b) SI (ions) and (c) pristine. (Right) PIXE for all the samples.

4. Conclusion

Experiments of electron and ion bombardment in HOPG were performed. A comparison between different incident particles was shown. Raman spectroscopy was used to characterize the structural features and defects produced by both impinging projectiles. The defect-induced D band, as well as the G and 2D bands were identified. Using a three-stage model for classifying defects in graphene, the defects were classified in a stage in which there is sp^2 clustering only, without sp^3 sites (Stage 1). SQUID measurements were performed after checking for contamination by PIXE. The obtained curves indicate ferromagnetic behavior in HOPG, increased by particle irradiation. The electron-irradiated sample shows a change in its magnetic properties with respect to the pristine sample which is increased with respect to the ion-irradiated sample. Further studies are being conducted in order to have a deeper insight into this issue.

5. Akcnowledgements

The authors thank Dr. Gustavo Castellano and Dr. Silvina Limandri, for carrying out the irradiation experiments, Dr. Cecilia Blanco for her suggestions concerning diffraction spectra analysis, and Dr. Luis Foa Torres for useful contributions to discussions. The authors also would like to thank FONCYT, Secyt-UNC and Conicet for financial support.

6. References

Allemand, P. M., Khemani, K. C., Koch, A., Wudl, F., Holczer, K., Donovan, S., Grüner,G., Thompson, J. D., 1991. Organic molecular soft ferromagnetism in a fullerene C60. Science 301, 301-302.

Compagnini, G., Puglsi, O., Foti, G. 1997. Raman spectra of virgin and damaged graphite edge planes. Carbon 35 (12): 1793-1797.

Eckmann, A., Felten, A., Mishchenko, A., Britnel, L., Krupke, R., Novoselov, K., Casiraghi, C., 2012. Probing the Nature of Defects in Graphene by Raman Spectroscopy. Nano Letters 12, 3925.

Esquinazi, P., Setzer, A., Höhne, R., Semmelhack, C., Kopelevich, Y., Spemann, D., Butz, T., Kohlstrunk, B., Lösche, M., 2002. Ferromagnetism in oriented graphite samples. Physical Review B 66, 429-453.

Esquinazi, P., Spemann, D., Höhne, R., Setzer, A., Han, K. H., Butz, T., 2003.Induced magnetic ordering by proton irradiation in graphite. Physical Review Letters 91, 227201.

Ferrari A. C. and Robertson, 2000. Raman spectroscopy of amorphous, nanostructured, diamond-like carbon, and nanodiamond. Physical Review B 61, 14096.

Iijima, S., 1991. Helical microtubules of graphitic carbon. Nature 354, 56-58.

Kopelevich, Y., Esquinazi, P., Torres, J. H. S., Moehlecke, S., 2000. Ferromagnetic- and superconducting-like behaviour of graphite. Journal of Low Temperature Physics 119, 691-702.

Kotakoski, J., Krasheninnikov, A. V., Kaiser, U., Meyer, J. C., 2011. From Point Defects in Graphene to Two-Dimensional Amorphous Carbon. Physical Review Letters 106, 105505.

Krasheninnikov, A. V., Nordlund, K., 2010. Ion and electron irradiation-induced effects in nanostructured materials. Journal of Applied Physics 107, 071301.

Makarova, T. L., Sundqvist, B., Höhne, R., Esquinazi, P., Kopelevich, Y., Scharff, P., Dadydov, V. A., Kashevarova, L. S., Rakhmanina, A. V., 2013. Magnetic carbon. Nature 413, 716-718.

Mizogami, S., Mizutani, M., Fukuda, M., Kawabata, K., 1991. Abnormal ferromagnetic behaviour for pyrolytic carbon under low temperature growth by CVD method.Synthetic Metals 43, 3271–3274.

Novoselov, K. S., Geim, A. K. , Morozov, S. V. , Jiang, D. , Zhang, Y. ,Dubonos, S. V. , Grigorieva, I. V. , Firsov, A. A. , 2004.Two-dimensional gas of massless Dirac fermions in graphene. Science 306, 666-669.

O'brien, S.C., Heath, J. R., Kroto, H. W., Curl, R. F., Smalley, R.E., 1986. A reply to "magic numbers in Cn^+ and Cn^- abundance distribution" based on experimental observations. Chemical Physics Letters 132, 99-102.

Pimenta, M. A., Dresselhaus, G., Dresselhaus, M. S., Cançado, L. G., Jorio, A., Saito, R., 2007. Studying disorder in graphite-based systems by Raman spectroscopy. Physical Chemistry Chemical Physics 9, 1276-1290.

Talyzin, A., Dzwilewski, A., 2007. Ferromagnetism in C60 polymers: pure carbon or contamination with metallic impurities? Journal of Nanoscience and Nanotechnology **7**, 1151-1161.

Xiaochang, M., Sefaattin, T., Hebard, A.F., 2012. Extinction of ferromagnetism in highly ordered pyrolytic graphite by annealing. Carbon 50, 1614-1618.